

STUDY ON THE MICROSTRUCTURAL CHANGES AND IMPACT ON THE PITTING CORROSION BEHAVIOUR OF 2507 DUPLEX STAINLESS STEEL WELD REGIONS

M Bassiouni¹, L P Ward¹, R K Singh Raman², A P O'Mullane³ and B Gideon⁴

¹School of Civil, Environmental and Chemical Engineering, RMIT University, Melbourne, Vic 3001, Australia. ²Department of Mechanical Engineering, Monash University, Melbourne, Vic. 3800, Australia. ³School of Applied Sciences, RMIT University, Melbourne, VIC 3001, Australia. ⁴ARV Offshore, Bangkok, Thailand.

Summary: The critical pitting temperature (CPT) test (ASTM G-150) is an electrochemical test generally used to evaluate the resistance of stainless steels to pitting corrosion, based on the concept of determining the potential - independent critical pitting temperature. Although this test has been done on the base metals of most stainless steels, few studies have been conducted on the weld regions, particularly the duplex stainless steels. In the present study, CPT and conventional potentiodynamic scanning tests were conducted on the various weld passes, namely root, filler and cap. Results were compared with the base material as a reference. The microstructure of the various weld regions, were characterised using optical microscopy, scanning electron microscopy and EDX analysis. The extent of degradation and the mechanisms responsible for pitting corrosion in terms of the various microstructural features within the different weld regions were examined. Variations in the microstructure was observed between the different weld regions in terms of ferrite/austenite ratio, grain shape and size and the formation of undesirable secondary phases such as chromium nitride and sigma phase. The CPT measurements revealed that the lowest pitting resistance was observed for the cap then the root pass; maximum corrosion resistance being observed for the base metal. Possible correlations between the microstructural changes and the pitting corrosion resistance of each region are discussed.

Keywords: Duplex Stainless Steel, SDSS, CPT, Pitting Corrosion.

1. INTRODUCTION

Duplex stainless steels such as AISI 2507 have found wide-spread use in industries, such as oil and gas production, pulp manufacturing, and power plants due to their high corrosion resistance and superior mechanical characteristics, where typical working environments can contain high levels of chloride attack with operating temperatures in excess of 100 °C [1]. These favourable properties arise from the coexistence of ferrite and austenite phases in equal amounts. Duplex stainless steels have higher strength than austenitic stainless steels, higher toughness than ferritic stainless steels, good weldability, and high resistance to different forms of corrosion in different aggressive environments [2, 3].

Superior corrosion performance of duplex stainless steels (DSS) is due to the alloying elements such as chromium, molybdenum and nitrogen, which increase the pitting corrosion and stress corrosion cracking resistance of these steels in a variety of environments [4]. However, limitations associated with this group of steels, particularly the weld regions, are the complex microstructural transformations that can occur, dissolution of ferrite, thus altering the ferrite / austenite (δ/γ) ratio and formation of secondary austenite and other undesirable chromium enriched intermetallic phases such as $M_{23}C_6$, sigma, chromium nitride, and chi phases. Such changes can be attributed to the rapid cooling involved in most weld thermal cycles. Consequently, alloy depleted regions associated with the formation of these phases may lead to a massive reduction in the corrosion resistance of the weld and make it more susceptible to different forms of corrosion such as pitting corrosion and stress corrosion cracking [4-7].

ASTM G-150, standard test method for electrochemical critical pitting temperature testing of stainless steels, is used for the evaluation of the resistance of stainless steel and related alloys to pitting corrosion in terms of measuring a potential independent critical pitting temperature (CPT) which might be defined as the lowest temperature on the test surface at which stable propagating pitting occurs under specified test conditions indicated by a rapid increase beyond a set limit of the measured anodic current density of the specimen[8].

Much research has been conducted primarily on the parent material and heat affected zones in terms of its susceptibility to various forms of corrosion and effects of addition of alloying elements. However there has been little research conducted on the corrosion characteristics and structural transformation of the weld metal in terms of the susceptibility to intergranular corrosion of the various successive weld layers namely the root, fill and cap layers [9].

The objective of the present study was (i) evaluate the characteristics of the microstructural transformations that have occurred in the different weld regions; (ii) measure the CPT for each weld region; (iii) conduct potentiodynamic scans to measure the pitting corrosion rate at different temperatures in chloride medium for each weld region and (iv) correlate the microstructural changes that have occurred to the pitting corrosion behaviour of these weld regions.

2. EXPERIMENTAL PROCEDURE

2.1. Material Specifications

SAF 2507 super duplex stainless steel metal plate (10 mm thickness) was used in this study. Multipass welding was carried out using standard gas tungsten arc welding (GTAW), and 2507 filler wire (AWS A5.9 "ER25.10.4.L). The chemical composition of the base metal and the employed filler materials as quoted by the supplier (Sandvik) are shown in Tables 1 and 2.

Table (1) Chemical composition for AISI 2507 duplex stainless steel plate

P (max)	S(max)	C(max)	N(max)	Si	Cr	Mn	Fe	Ni	Mo	Total
0.035	0.015	0.03	0.3	0.8	25	1.2	61.67	7	4	100

Table (2) Chemical composition used for the 2507 filler wire

C	Cr	Ni	Mo	N	Mn	Si	Fe
0.02	25	9.5	4	0.25	0.4	0.35	Rest

2.2. Microstructural Evaluation

ASTM A923 method A was employed to confirm the existence of intermetallic phases in the sensitised material and their absence in the unsensitised samples [10, 11]. Test specimens were initially mounted, ground and polished to 3µm using standard metallographic preparation techniques. Samples were then electrochemically etched in a 40% NaOH solution at 3V for 15-60 seconds. The resultant microstructure was evaluated using optical light microscopy (OLM) and scanning electron microscopy (SEM), specifically the FEI Nova Nano-SEM (2007) with EDAX Si (Li) X-ray detector.

2.3. Pitting Corrosion Study using ASTM G-150 test

The tests were carried out according to the ASTM G150 procedures [12]. The test method determines the potential independent critical pitting temperature (CPT) by way of a potentiostatic technique using a temperature scan (see Fig. 1). The specimen's exposed surface was immersed in the test solution of 1M NaCl, initially at 0°C. After an initial temperature stabilization period, the solution was heated at a rate of 1°C/min. About 60 s before the temperature scan was commenced, the specimen was anodically polarized to a potential above the pitting potential range (a potential of 700 mV vs 3M Ag/AgCl reference electrode was found to be suitable for most stainless steels and was employed in the current study) [7]. This potential was held constant during the whole temperature scan. The current was monitored during the temperature scan, and the CPT was defined as the temperature at which the current increases rapidly, which for practical reasons is defined as the temperature at which the current density exceeds 100 µA/cm² for 60 s [8]. Pitting of the specimen and absence of crevice corrosion were confirmed visually after the test using OLM.

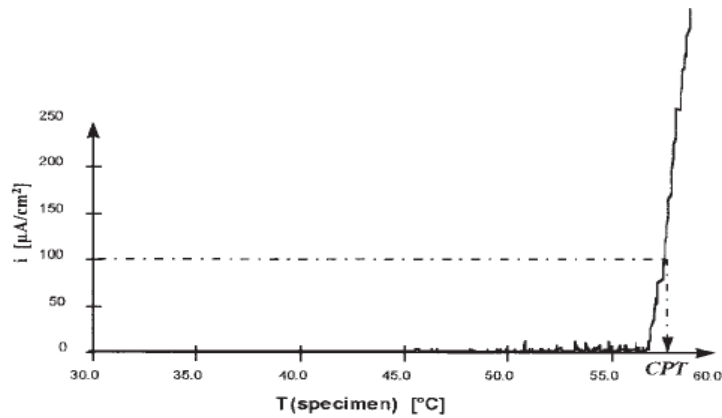


Figure 1 Principal of CPT test [8]

2.4. Potentiodynamic scanning tests

Potentiodynamic scans on the different weld regions and the base metal are conducted using a Voltalab 21 potentiostat. Scan range varied from a cathodic maximum of -500 mV to an anodic maximum of +200 mV. The reference electrode was a 3M Ag/AgCl electrode. Scan rate employed was 1.67 mV/sec. Tests were conducted at 20 °C and 83°C respectively. Corrosion rates (i_{corr} values) were determined by Tafel extrapolation, calculated from the Voltmaster software. A typical potential vs. Log current density plot showing Tafel extrapolation from this software is shown in Figure 2.

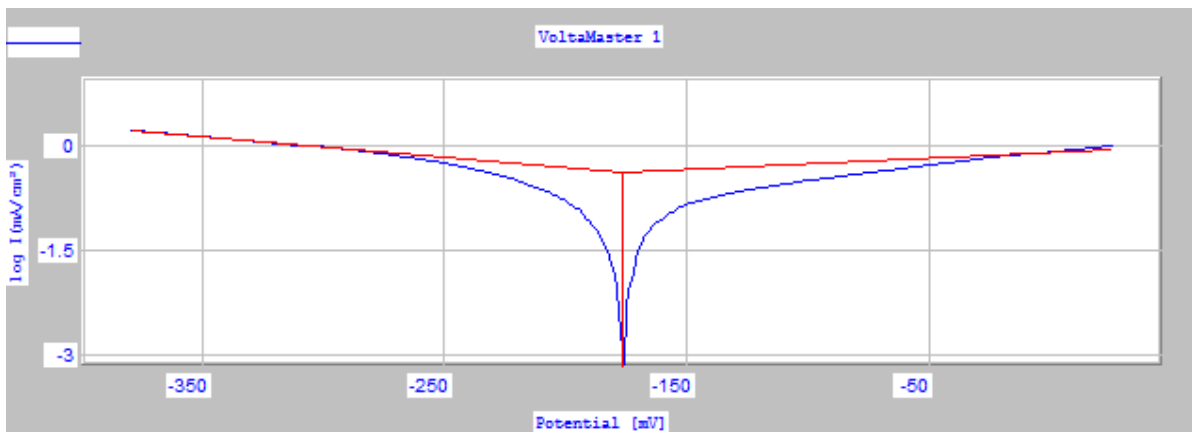


Figure 2 Example of the obtained result

3. RESULTS

3.1. Microstructure Evaluation

The macro structure appearance of the weld joint, base metal, and different weld passes are shown in Figure 3. Engraved light gray area at the right represent the weld joint consist of the cap pass at the top, followed by the filler pass, then finally the root pass at the bottom. While the flat dark gray area represent the base metal.

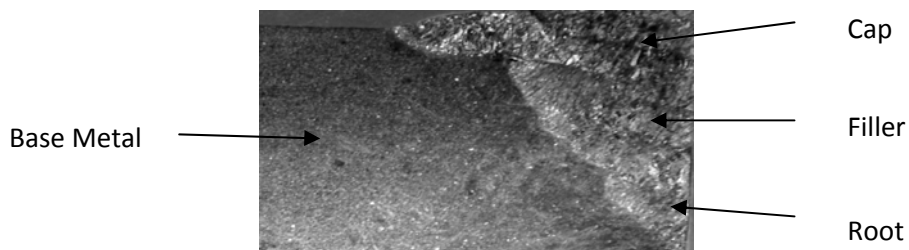


Figure 3 Macro structure appearance of half weld joint

3.1.1. Base metal

Figure 4 shows a SEM of the base metal where the microstructure consists of equal amounts of elongated ferrite and austenite grains. Here, the dark regions are associated with the presence of ferrite and the bright regions with austenite. Identification of these two phases based on EDXS analysis (Figure 5) are quantified in Table 3. The ferrite phase contains a higher concentration of ferrite promoting elements such as Cr, and Mo. Likewise, the austenite phase contains a higher concentration of austenite promoting elements such as Mn, Ni, and nitrogen. The volume fraction of ferrite and austenite in the base metal was determined using standard test procedures according to ASTM E-562 [13]. The obtained results (Table 4) confirmed the coexistence of an almost equal amount of ferrite and austenite phases in the base metal.

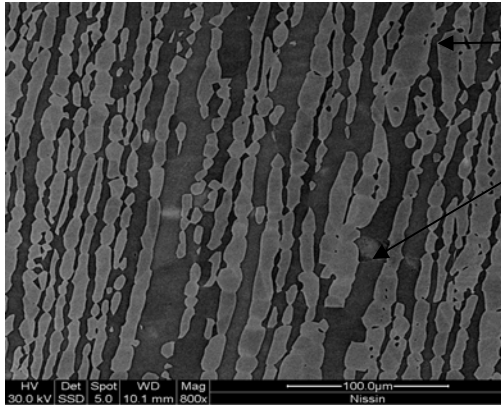


Figure 4 Microstructure of etched SAF 2507 base metal

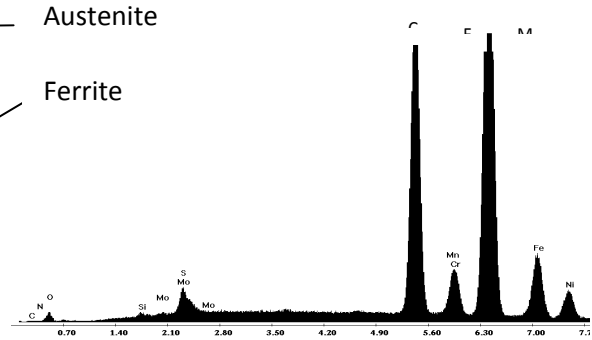


Figure 5 Qualitative EDXS analysis for the SAF 2507 Base metal

Table 3 Chemical composition of austenite and ferrite phases

	P	S	C	N	Si	Cr	Mn	Fe	Ni	Mo	Total
Ferrite	0	0	0	0	0.71	25.63	0.85	61.3	5.96	5.55	100
Austenite	0	0	0	0.23	0.64	23.41	0.92	62.35	8.28	4.17	100

Table 4 Volume fraction of ferrite and austenite in the base metal

	Austenite	Ferrite	Total
Total Area (mm²)	0.86	0.78	1.64
%	51.83	48.17	100

3.1.2. Weld Fusion Zones

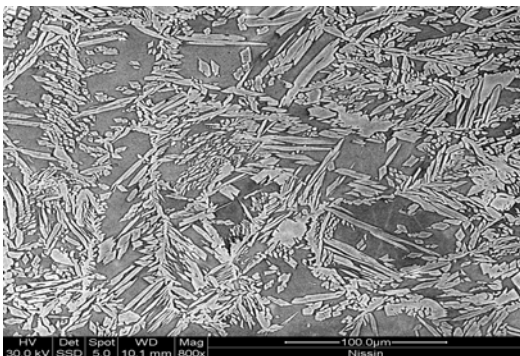


Figure 6 Microstructure of etched SAF 2507 root weld region (X800)

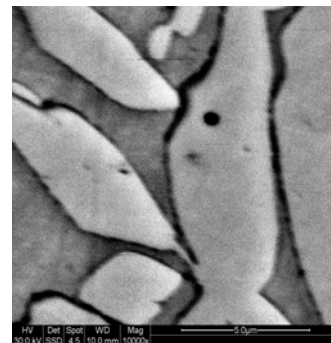


Figure 7 Microstructure of etched SAF 2507 root weld region at higher magnification (X 10,000)

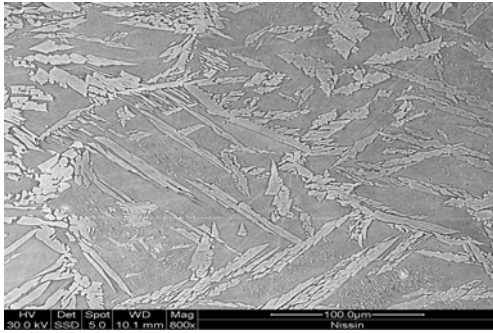


Figure 8 Microstructure of etched SAF 2507 filler weld region (X800)

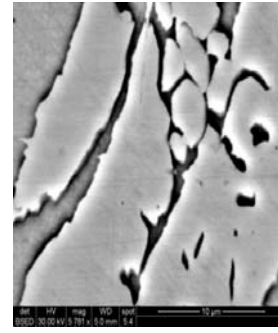


Figure 9 Microstructure of etched SAF 2507 filler weld region at higher magnification (X 5,780)

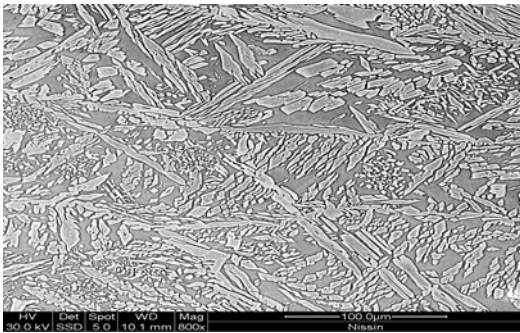


Figure 10 Microstructure of etched SAF 2507 cap weld region (X800)

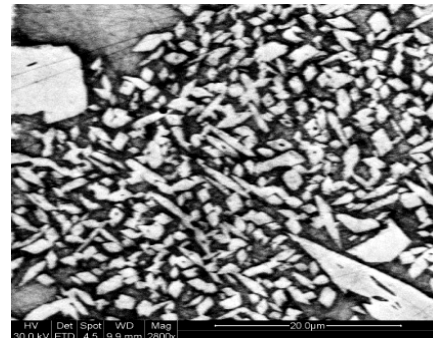


Figure 11 Microstructure of etched SAF 2507 cap weld region at higher magnification (X2800)

In general, the austenite regions in the DSS weld metal is formed from ferrite in three modes, as allotriomorphs at the prior-ferrite grain boundaries, as Widmanstätten side-plates growing into the grains from these allotriomorphs and as intragranular precipitates. Similar observations have been reported elsewhere [14].

For the different weld regions figure 6-11, elongated platelets of allotriomorphic and wedge shaped Widmanstätten austenite in ferrite matrix are clearly seen. In addition, intergranular intermetallic precipitates formed at the ferrite/austenite grain boundaries and idiomorphic secondary phases (possibly sigma, or Chi phases) within the austenite grains are observed.

The root region shows a large amount of allotriomorphic ferrite, Widmanstätten-ferrite and non-lamellar ferrite is evident, which may be due to the higher degree of cooling. In the root region, the observed structure mainly consisted of grain boundary allotriomorphs, large elongated platelets and small fine, equiaxed dendritic regions, surrounded by fine discontinuous regions of ferrite. However, the austenite seen within the grain could be associated with either intragranular precipitates or Widmanstätten austenite.

Large regions of ferrite were observed in the fill regions, which consisted of elongated bands of austenite surrounded by ferrite as well as intragranular precipitates. Normal grain growth was observed predominantly in these regions of the weld, characterised by the development of austenite, associated with Widmanstätten type structures dominating the observed morphology. The development of these growth mechanisms can be attributed directly to the variations in the degree of under cooling, where there is a higher degree of under cooling occurring within the cap region as opposed to the fill region.

The cap region shows smaller continuous regions of ferrite, in addition to some intragranular precipitates. Widmanstätten side plates and grain boundary allotriomorphs were observed to be the dominant morphologies. Analysis of the cap region at higher magnifications reveals a structure consisting of small grains of ferrite, secondary austenite, intermetallic precipitates, and secondary phases.

3.2. Electrochemical Corrosion Tests

3.2.1. Critical Pitting temperature measurements

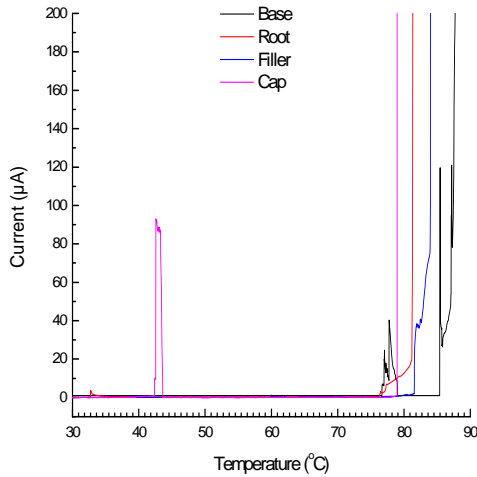


Figure 12. Current vs temperature plot for the different weld regions

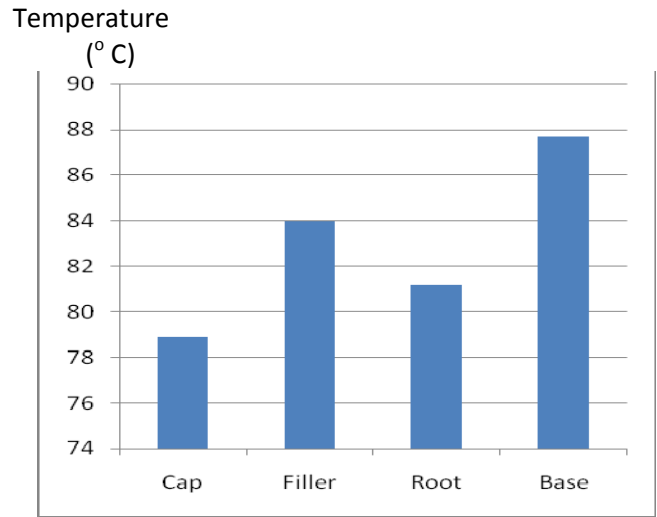


Figure 13. CPT for the different weld regions

Figure 12 shows the current versus temperature plot for the different weld regions. During a typical test, the passive current density was less than $1\mu\text{A}$ for most of the test. However, a few small spikes would be seen as the CPT was approached. Figure 13 shows the CPT values for the different weld regions.

The lowest CPT values were observed for the cap and root regions (79 and 81 °C respectively) compared with the filler and base regions yielding CPT values of 84 and 87.5 °C). This has been proved by the obtained corrosion rate measured at 20 °C and 83 °C as discussed below.

3.2.2. Corrosion rate measurements

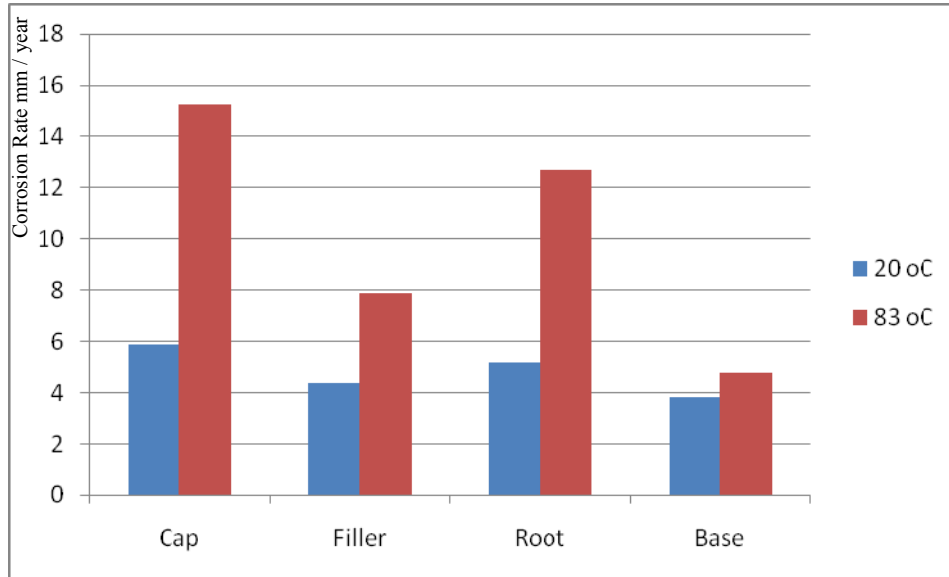


Figure 14. Corrosion rate values for the different weld regions

Figure 14 shows corrosion rate for the different weld regions measured at 20 °C and 80 °C in 1 M NaCl. Higher corrosion rates were observed for tests conducted at 83 °C compared to 20 °C, for any given region, However, the difference in the two values at the different vs temperatures was much less for the base and filler compared with the root and cap regions. In particular, the corrosion rate of the base metal at 20 °C was very similar to that measured at 83 °C. Consequently, some correlations can be drawn between the CPT and potentiodynamic scanning studies. Generally, potentiodynamic scanning studies conducted below the critical pitting temperature induced lower corrosion rates than those conducted above the CPT. The elevated CPT for the base material, which was greater than the temperatures at which both the potentiodynamic scans were conducted at, may be responsible for the little variation observed in the corrosion rates. However, the large difference observed for the tests conducted on the cap region can be attributed to the fact that the lower temperature test was conducted below the CPT, whereas the higher temperature study was conducted above the CPT.

4. DISCUSSION

4.1. Microstructure Evaluation

Analysis of the base metal microstructure revealed the presence of a two-phase banded structure typical of such materials. It consists of large elongated lath type ferrite and austenite regions in equal proportions. This has been attributed to the processing of the base metal where rolling of the plate has resulted in the production of elongated phases. However, the structures observed in the weld regions were quite different to those observed in the base material. Variations in the observed microstructures and relative distributions of the austenite and ferrite regions can be observed not only between the base metal and weld regions, but between the different weld regions themselves. Similar observations have been observed elsewhere[15].

The welding of duplex stainless steels is known to induce microstructural changes resulting in the formation of unbalanced austenite/ferrite ratios compared with the base material. In addition, austenite can be present as intergranular, intragranular and secondary austenitic. Such transformations are accompanied by high rates of cooling and production of weld structures with higher ferrite contents in the filler and root [16] and formation of a coarsened ferrite structure in the cap region[14].

For all weld pass regions, the possible presence of, fine intermetallic precipitates were observed between the ferrite and austenite grains and secondary phases (possibly sigma or chi phases) within the austenite grains. The presence of such precipitates has been known to lead to significant reduction in the mechanical properties and corrosion behaviour of these weld regions [7]. However, the specific composition of these precipitates could not be identified from the current facilities available as the sizes of the precipitates were too small and hence this precluded identifying the type of precipitate present. However previous studies [17] have observed similar findings and reported that such observed features have been attributed to the presence of chromium nitride and sigma phases. Scanning electron microscopy has revealed that the size of the precipitates are generally in the range 1 μm to 2 μm . However, the overall percentage content of precipitates cannot be accurately determined using current analytical facilities. Accurate determination of size and distribution of precipitates require other more sophisticated analytical techniques (image analysis with appropriate software or TEM). This analysis is for future work.

4.2. Electrochemical Tests

The CPT, as determined by the ASTM standard method, is primarily a reflection of the conditions for initiation of a “stable” pit provided that the initiated pit, or pits, can generate a current equivalent to 100 $\mu\text{A}/\text{cm}^2$ averaged over the surface area of the specimen.

It is quite likely that the CPT is determined by the extent of alloying element depletion, particularly if there is a localised region of severe depletion and other induced microstructural features. The possible formation of chromium rich intermetallic precipitates and secondary phases in the different weld regions are likely to result in the existence of chromium depleted regions that may reduce the pitting corrosion resistance of the different weld regions compared to the base metal. Additionally, shifts in the austenite/ferrite ratio as a result of different heating/cooling cycles associated with the welding process, can strongly influence the pitting corrosion resistance. The base metal, followed by the fill region, shows the highest CPT, which might be due to the austenite/ferrite phase balance. The reduced amount of austenite observed in the fill region (Figure 8) compared with the cap and root region (Figures 6 and 10) may be responsible for the increased CPT of the fill region. Increased levels of austenite observed in the root and cap regions may be responsible for the reduced CPT's. Generally, the lower observed CPT values for the weld regions compared to the base metal may be attributed to the possible presence of intermetallic precipitates, which are absent in the base material.

5. CONCLUSIONS

1. The critical pitting temperature (CPT) test (ASTM G-150) was successfully applied to study the base material and various weld regions within a 2507 grade super duplex stainless steel welded plate.
2. Differences in the microstructural features were not only observed between the base metal and the weld region, but between the different weld regions themselves. This may be associated with different thermal cycles and subsequent different cooling rates associated with the welding process. This resulted in different ferrite / austenite ratios being observed, in addition to the presence of secondary austenite and possible intermetallic phases within the weld regions

3. The critical pitting temperature was shown to be a maximum for the base material and lowest for the cap region. The CPT was observed to be strongly influenced by the microstructure, such as ferrite/austenite ratio, grains shape and size, and the presence of chromium rich intermetallic precipitates and secondary phases.
4. The pitting corrosion resistance (elevated CPT) was observed for the weld regions with increased ferrite (fill region). Likewise, increased amounts of austenite (cap and root) were accompanied by a reduction in the CPT.
5. Correlations were observed between the CPT studies and potentiodynamic scans at different temperatures. Lower corrosion rates were observed for studies conducted at temperatures lower than the CPT. Large differences were observed for the regions where the lower temperatures studied were below the CPT and the higher temperatures studied above the CPT. In contrast, corrosion rates for the base material were similar as both temperatures studied were lower than the CPT.
6. The CPT appears to be influenced by microstructural features such as the austenite / ferrite ratio and the presence of intermetallic phases, resulting in alloying element depleted regions. Future work in this area is recommended for a more detailed systematic examination of the microstructural features and influence on CPT, to include variations in chemical composition, volume fraction of precipitates and detailed evaluation of the intermetallic precipitates and secondary phases.

6. ACKNOWLEDGEMENTS

The authors would like to acknowledge the technical guidance and support from Mr. Phil Francis, Mr. Peter Rummel, and Mr. Mike Allen from RMIT University.

7. REFERENCES

1. Bastos, I.N. And R.P. Nogueira, *Electrochemical Noise Characterization Of Heat-Treated Superduplex Stainless Steel*. Materials Chemistry And Physics, 2008. 111.
2. Badji R, Bouabdallah M, Bacroix B, Kahloun C, Belkessa B and Maza H, Phase transformation and mechanical behavior in annealed 2205 duplex stainless steel welds *Materials Characterization*, 59 (4) (2008) 447-453
3. B. Gideon, L.P. Ward and G. Biddle, Duplex Stainless Steel Welds and their Susceptibility to Intergranular Corrosion. *Minerals and Materials Characterisation and Engineering* 7 (3) (2008) 247 – 263
4. Bhattacharya A and Singh PM, Stress corrosion cracking of duplex stainless steels in caustic solutions, *Journal Failure Analysis and Prevention* 7 (5) (2007) 371-377.
5. Amadou, T., H. Sidhom, And C. Braham, *Double Loop Electrochemical Potentiokinetic Reactivation Test Optimization In Checking Of Duplex Stainless Steel Intergranular Corrosion Susceptibility*. Metallurgical And Materials Transactions, 2004. 35 A: P. 15.
6. Wen S, Lundin CD and Baten G, Metallurgical evaluation of cast duplex stainless steels and their weldments, Final report Vol. 1 submitted to US Department of Energy, Award Number - DE-FC36-00 ID13975, 2001.
7. Turnbull A, Francis PE, Ryan MP, Orkney LP, Griffiths AJ and Hawkins B, A novel approach to characterizing the corrosion resistance of super duplex stainless steel welds. *Corrosion (NACE)* 58 (12) (2002) Paper No 02121039
8. Baboian R (Ed), Corrosion tests and standards: application and interpretation (In) ASTM manual series, MNL 20-2ND, West Conshohocken, PA, ASTM International, 2004
9. B Gideon B and L Ward, Intergranular corrosion and residual stress determination of a duplex stainless steel pipeline girth weld (In) *Proc. Corrosion & Prevention*. Nov 16-19, 2008, Wellington, New Zealand, Paper 110
10. Astm, A923-94 "*Standard Test Methods For Detecting Detrimental Intermetallic Phase In Wrought Duplex Austenitic/Ferritic Stainless Steels*".
11. Russell SW and Lundin CD, The development of qualification standards for cast duplex stainless steel, Final report, Vol. 2 submitted to US Department of Energy, Award Number - DE-FC36-00 ID13975, 2005
12. ASTM, G150, "*Standard Test Method for Electrochemical Critical Pitting Temperature Testing Of Stainless Steels*". 1999.
13. ASTM, E562 *Standard Test Method For Determining Volume Fraction By Systematic Manual Point Count*.
14. Gideon, B., L. Ward, And G. Biddle, *Characterisation Of Duplex Stainless Steel Welds And Their Susceptibility To Intergranular Corrosion*, In *Euro Corr I*. 2006.
15. Gideon B, Structural characterisation, residual stress determination and degree of sensitisation of duplex stainless steel welds, Ph.D Thesis, School of Civil, Environmental, and Chemical Engineering, RMIT, 2009, p. 265.
16. Yuan, X., C.Y. Kang, And M.B. Kim, *Microstructure And Xrd Analysis Of Brazing Joint For Duplex Stainless Steel Using A Ni-Si-B Filler Metal*. Elsevier Inc., 2009: P. 9.
17. Magnabosco R, Kinetics of sigma phase formation in a duplex stainless steel, *Materials Research* 12 (2009) 12 7.

8. AUTHOR DETAILS

 A portrait of Mohamed Bassiouni, a man with dark hair and a mustache, wearing a light purple shirt and a patterned tie, set against a blue background.	<p>Mohamed Bassiouni Post Graduate Student within the School of Civil, Environmental and Chemical Engineering, RMIT University. Currently holds the position of Process Engineer within Lycopodium Process Industries Pty Ltd – Melbourne – Australia. Prior to this he has extensive experience in industry since 2000. Research interests are focussed predominantly in the area of Corrosion behaviour and weld integrity of duplex stainless steel.</p>
 A portrait of Dr Ward, a man with light brown hair, wearing a yellow shirt and a blue patterned tie, set against a light blue background.	<p>Dr Ward currently holds the position of lecturer within the School of Civil, Environmental and Chemical Engineering, RMIT University, since 1996. Prior to this he was currently employed at the University of South Australia. His background is in Metallurgy and Materials Engineering, having obtained his Ph.D. in the development of PVD coatings for orthopaedic applications from Newcastle Polytechnic, UK, in 1991. Research interests are focussed predominantly in the area of surface engineering, specifically structural characterisation, corrosion and wear behaviour and surface modification using ion implantation. More recently, interests have extended to corrosion behaviour of Al alloys for aerospace applications and weld integrity of duplex stainless steels</p>
 A portrait of R. K. Singh Raman, a man with dark hair and glasses, wearing a white striped shirt and a dark tie, set against a light blue background.	<p>R. K. Singh Raman is an Associate Professor in the Department of Chemical Engineering and Department of Mechanical & Aerospace Engineering at Monash University. His research interests are in: (a) Role of alloy nano- / microstructure in corrosion of ferrous and light alloys, (b) High temperature gaseous corrosion of steels and weldments, (c) Stress corrosion cracking of steels, their weldments and light alloys, (d) Stress corrosion cracking monitoring techniques, (e) Corrosion of magnesium alloys and (f) Corrosion resistance advanced coatings and paints. He has supervised 16 PhD and 4 Masters students in the area of corrosion, and published over 100 peer-reviewed journal papers and over 80 reviewed conf papers.</p>



Dr. O'Mullane is currently a postdoctoral fellow in the School of Applied Sciences and the Platform Technologies Research Institute, RMIT University. His background is electrochemistry having obtained his PhD in 2001 from University College Cork, Ireland. His research interests are the electrochemical synthesis and characterisation of nanostructured materials, electrocatalysis, semi-conducting charge transfer complexes and the application of electrochemical methods to various aspects of materials science.



Dr Gideon, is currently Proprietor and Principal Consultant at CORRMET LTD. His background is welding metallurgy, non-destructive testing and materials engineering for the oil and gas industry. He obtained his Ph.D. in characterisation, residual stress determination and sensitization of duplex stainless steel welds in 2009 from RMIT University. His research interests are in: (a) Application of stainless steels and nickel alloys in oil and gas industries, (b) Phase transformation of alloys, (c) Intergranular corrosion and stress corrosion cracking of steels, and (d) Residual stress determination by neutron diffraction,